Physical Model of District Heating Networks to Boost the Transition to Next-Generation Systems

IIETA International Information and Engineering Technology Association
Advancing the World of Information and Engineering

Mathematical Modelling of Engineering Problems
Vol. 12, No. 10, October, 2025, pp. 3427-3434
Journal homepage: http://iieta.org/journals/mmep

Physical Model of District Heating Networks to Boost the Transition to Next-Generation Systems

Martina Capone

Energy Department, Politecnico di Torino, Torino 10129, Italy

Corresponding Author Email: martina.capone@polito.it

https://doi.org/10.18280/mmep.121009

Received: 11 September 2025
Revised: 19 October 2025
Accepted: 25 October 2025
Available online: 31 October 2025

Keywords:
district heating, simulation model, smart energy systems, validation, 4GDH

ABSTRACT

District heating networks are key players in the decarbonization of urban energy systems. A detailed understanding of their thermo-fluid dynamic behavior is required to address their evolving operating conditions, such as lower temperature supply, increasing integration of storage and renewable energy sources, and the interconnection with the electricity grid. In this scenario, the development and application of simulation models to estimate the distribution and evolution of pressures, mass-flow rates, and temperatures along the networks is becoming increasingly important. In this work, a physical simulation model is proposed. This allows replicating the operation of the network under varying operating conditions, making it possible to simulate potential future scenarios. The compactness of the model allows large-scale networks to be simulated without excessive computational effort. Moreover, a compact simulation setup allows the simulation model to be incorporated into optimization frameworks, which are essential in a transition context where a large number of changes have to be tested and implemented. The methodology is applied to a real large-scale district heating network, providing insights into the thermo-fluid dynamics of the network and enabling the assessment of system responses under varying boundary conditions. The results highlight how physically accurate and computationally efficient simulation tools can facilitate the transition towards more sustainable energy systems.

1. INTRODUCTION

District heating systems (DHS) are widely recognized as a key technology for the decarbonization of the energy system [1]. Despite being a well-established technology, adopted in Europe since the late 19th century, DHS are currently experiencing a significant transformation. Early systems were primarily supplied by fossil fuels and operated at high temperatures to maintain relatively low circulating mass flow rates. Contemporary DHS, in contrast, are increasingly recognized as critical enablers of the energy transition [2, 3], facilitating the integration of renewable energy sources and waste heat, and enabling the distribution of this low-carbon heat to wide urban areas [4, 5].

This fundamental change in operational paradigm necessitates deep modifications that existing infrastructures may not fully support [6]. These limitations can manifest on the consumer side, with radiators designed for high-temperature operation and thermal substations with limited heat exchanger surface areas, and in the distribution infrastructure, with pipe dimensions that may be inadequate to accommodate the higher mass flow rates associated with lower temperature operation [7].

However, a substantial number of DHS currently in operation were designed and built to operate with the older, high-temperature and fossil-fuel-based operational logics. To achieve a cost-effective decarbonization of the broader energy system, it is therefore essential to adapt these existing infrastructures to the new operational conditions, avoiding the substantial expenditure associated with a complete redesign and substitution of these systems.

Enabling the transition of these older-generation systems requires robust tools and methodologies to accurately assess their performance and behavior under the evolving operational demands [8]. The development and application of detailed simulation models is thus taking on a growing relevance, as these models allow for testing of possible modifications to the systems before physical implementation, obviating the need for expensive and often logistically challenging experimental tests [9, 10]. This capability is of particular importance in a context where a large and complex set of modifications must be evaluated and potentially implemented, including: the increasing integration of renewable energy sources and waste heat; the deployment of thermal energy storage (TES); the integration of prosumers into the network; a shift towards more distributed heat production; the reduction of operating temperatures; and the interconnection with other energy networks, such as electricity grid [11].

In this context, this paper aims to propose an accurate model to assess the evolution and distribution of pressures, mass flow rates and temperatures in the distribution infrastructure under varying conditions. The goal is to introduce a tool capable of

predicting the behavior of the district heating network when the operating conditions are modified to adapt to the system transition.

To evaluate the reliability of the proposed model, it is applied to a real large-scale case study. A comparison between the model results and experimental measurements allows for the validation of the proposed methodology.

2. METHODOLOGY

This section outlines the methodology adopted to simulate the dynamics of the DHS. Firstly, a brief review of the main characteristics of the modeling strategies in the literature is presented, followed by a detailed description of the model adopted in this study.

From a literature review, it emerges that both physics-based and black-box data-driven models have been adopted to simulate the operation of DHS [12]. In this work, a physics-based approach is adopted due to its greater adaptability to diverse and evolving conditions typical of transition scenarios, where operational changes have not been previously tested and corresponding data are unavailable for training data-driven models.

Physics-based models rely on solving the conservation equations of mass, momentum, and energy. These equations have been addressed with different formulations in literature:

- Steady-state formulations were adopted by early models [13, 14] and continue to be used for planning and strategic decisions [15, 16];
- Fully transient formulations are usually limited to specific cases, such as the analysis of water hammer effects [17], due to their significant computational requirements;
- Pseudo-transient approaches are typically preferred by many authors [17-19]. In these models, pressure dynamics are often treated as quasi-steady since pressure perturbations propagate at the speed of sound in water, stabilizing rapidly. In contrast, temperature variations, which travel at the much slower flow velocity, are modeled dynamically to capture thermal transients effectively. This approach allows for accurate simulation of temperature behaviors without the computational overhead associated with fully dynamic models. For the mentioned advantages, this approach is adopted in this study.

Finally, the conservation equations have been solved in the literature using both Lagrangian and Eulerian approaches. In the Lagrangian approach, the model tracks the temperature evolution of discrete plug elements of water as they flow along the pipeline. In contrast, the Eulerian approach calculates the temperature profile by dividing each pipe into multiple fixed spatial segments and solving the equations at these discrete locations. This is preferred in this study to have a more detailed representation of the temperature distribution across the entire network.

The main characteristics of the physical model were previously discussed in study [20]: it is a one-dimensional FV approach, based on the solution of the integrated form of mass, momentum, and energy conservation equations, respectively reported in Eqs. (1)-(3). Each pipe is modeled as a branch of a graph, connecting an inlet node to an outlet node, according to the graph theory. The interconnections of pipelines and nodes are taken into account by means of the incidence matrix A: each row of the matrix corresponds to a node of the network, and each column to a pipe/branch; the various entries are equal to 1 if the node is the inlet node of the corresponding pipe, -1 if it is the outlet node, and zero if node and pipe are not related to each other.

$$\boldsymbol{AG} + \boldsymbol{G_{ext}} = \boldsymbol{0} \tag{1}$$

$$\boldsymbol{A^T P} + \rho g \boldsymbol{A^T z} = \boldsymbol{RG} - \boldsymbol{t} \tag{2}$$

$$(\boldsymbol{M} + \boldsymbol{K})\boldsymbol{T^t} = \boldsymbol{f} + \boldsymbol{MT^{t-1}} \tag{3}$$

The model is applied sequentially to the supply and return networks. The unknowns in the problem are the vectors $\boldsymbol{G}$, $\boldsymbol{P}$, and $\boldsymbol{T}$, which represent, respectively, the mass flow rates in the $\boldsymbol{NB}$ branches, the pressures in the $\boldsymbol{NN}$ nodes, and the temperatures in the NN nodes. Boundary conditions include: specified mass flow rates entering or leaving the system (with injections from the plants and extractions by users in the supply network, and vice versa in the return network), included in the vector, a prescribed pressure at one boundary node, and temperature conditions at the injection nodes. TES operates dynamically, acting as users during their charging phase and as plants during their discharging phase. An initial condition must be specified for the temperature at each node, as the thermal problem is transient.

The pumps are modeled as external head sources and included in the vector $\boldsymbol{t}$. $\boldsymbol{R}$ is a diagonal matrix (size $NB \times NB$) that accounts for the pressure losses, as expressed by Eq. (4).

$$R_{j,j} = \frac{1}{2}\frac{|G_j|}{\rho S_j^2}\left(f\frac{L_j}{D_j} + \sum\beta_j\right) \tag{4}$$

The system of equations represented by Eqs. (1)-(3) can be solved to determine the temporal and spatial behavior of the mass flow rates ($\boldsymbol{G}$), pressures ($\boldsymbol{P}$), and temperatures ($\boldsymbol{T}$) within the district heating network. Because mass flow rates and pressures are interrelated, Eqs. (1) and (2) cannot be solved independently in networks with loops; instead, a coupled approach is necessary. One effective method is to use the iterative SIMPLE algorithm, as proposed by previous studies [12]. This approach introduces non-linearity into the fluid dynamic model, which in turn necessitates the use of Mixed-Integer Nonlinear Programming (MINLP) techniques when integrating the model into optimization frameworks.

Alternatively, in this work a new solution strategy is proposed: the unknowns of the problem can be treated as fictitious decision variables within a feasibility optimization problem. By employing appropriate approximations, the problem can be reformulated as a Mixed-Integer Quadratically Constrained Program (MIQCP), solvable by commercial optimization software such as Gurobi, adopted in this study. This reformulation can substantially reduce computational times compared to the iterative SIMPLE solution, particularly when embedded within broader optimization tasks.

To speed up the computational solution, the mass flow rates in tree-shaped areas, that are not dependent on the pressure distribution, can be calculated within a pre-processing step in which Eq. (1) is solved independently from the pressure distribution in those areas. This pre-processing reduces the dimensionality of the problem by excluding mass flow rates in tree-shaped regions from the set of optimization variables, limiting them to only those branches involved in network loops.

Overall, the proposed simulation framework is based on the solution of a feasibility MIQCP problem, where $\boldsymbol{G}$, $\boldsymbol{P}$, and $\boldsymbol{T}$ are in the form of decision variables, and Eqs. (1)-(3) are in the form of constraints.

The same framework can be readily extended to an actual optimization problem by introducing appropriate degrees of freedom and defining an objective function to minimize. For instance, one possible application is optimizing the operation of the various pumps in order to reduce the overall hydraulic pumping power. This optimization framework can be adopted to support analyses relevant to the DHS transition scenario, enabling a more efficient system operation.

In this paper, the focus is on the simulation, in order to validate the model on complex DHS involving large infrastructures with multiple loops, multiple producers, and multiple TES systems. The validation process requires sufficient experimental measurements: in particular, the evolutions of pressures and temperatures resulting from the simulation are compared to the measurements in this analysis.

3. CASE STUDY

To evaluate the performance and reliability of the proposed modeling framework, it is applied to a real DHS located in Northern Italy. The system supplies thermal energy primarily for space heating across a large urban area, serving more than 8000 buildings with a total heated volume exceeding 75 million cubic meters. The demand for domestic hot water is limited, involving only a small share of the connected users.

The heat supply infrastructure is composed of multiple production units distributed throughout the city, as represented in Figure 1. These include three combined heat and power (CHP) plants, a waste-to-energy plant, and some auxiliary heat-only boilers that operate during peak load conditions. These plants are represented in the figure with red dots. In addition, thermal storage systems (TES) are installed at five different locations to improve load management and enhance operational flexibility. TES are represented in the figure with yellow triangles. During winter operation, the supply temperature in the network is maintained at approximately 120°C.

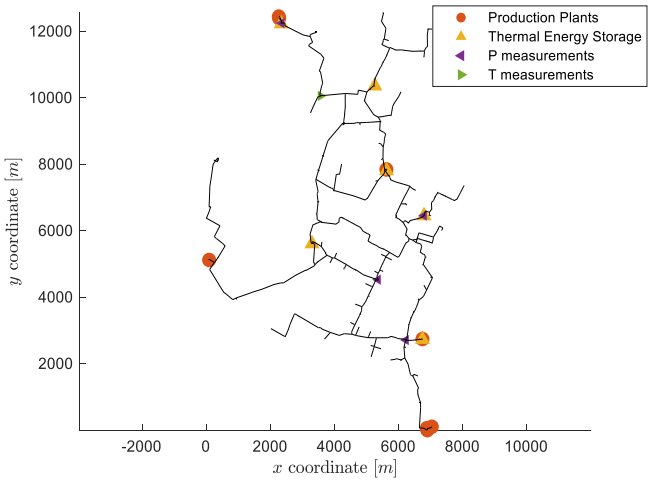

Figure 1. Schematic representation of the DHS, including the location of thermal plants, thermal energy storage units, and measurement points used for model validation

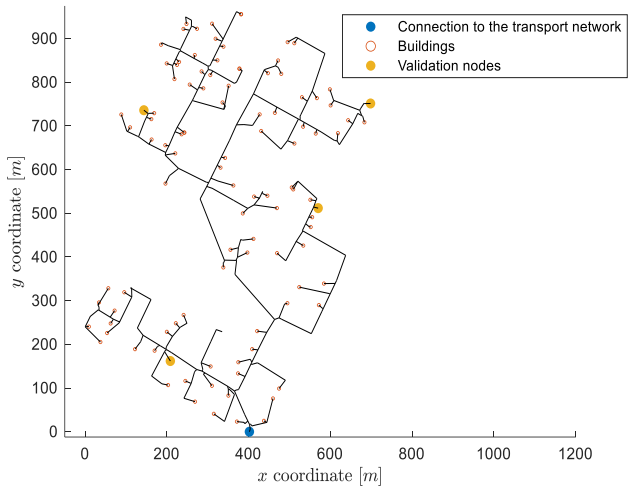

Figure 2. Schematic representation of one of the distribution networks connected to the transport network

Figure 1 also highlights the locations where measurement data are available. The fluid-dynamic model is validated using pressure measurements from three nodes; although four measurement points are shown, one is used to impose a boundary condition. The thermal model, on the other hand, is validated using a single temperature measurement located in the northern section of the network. Instead, temperature readings at the plant outlets are employed to define appropriate boundary conditions for the thermal simulation.

Figure 1 only shows the transport network, which represents the main backbone of the network. It involves large pipes that connect supply plants to various zones of the city via a pipe infrastructure with larger diameters. There are also many distribution networks with smaller pipes that connect the transport network to buildings in various neighborhoods: an example is the distribution network shown in Figure 2. In the first part of this analysis, the model is only applied to the transport network, but the same model structure can be adopted to simulate distribution networks. The topology of the transport network is represented through a graph with 918 nodes and 931 branches.

To simulate the transport network, the following information must be available (listed here for the supply network; a similar approach applies to the return network):

a) Mass flow rates injected by the various production plants and TES units during discharging phases. This data is provided by the DHS operator at a time resolution of 10 minutes.
b) Mass flow rates extracted by each distribution network and by the TES units during charging. With the exception of the TES units, this information is not directly available. It is estimated by distributing the total injected flow rate among the distribution networks according to their nominal design flow rates.
c) Pumps operation. These are provided by the DHS operator. If unavailable, different pump configurations can be tested. Note that pumping stations are present both at plant level and within the DHS.
d) Pressure at a reference node, required to set a pressure baseline. This value is obtained from available measurements.
e) Supply temperatures at the plant outlets. In some plants, an accurate time evolution of the supply temperature is

available to the authors, whereas in others, it is estimated based on average values. This introduces additional complexity in the thermal validation process. Moreover, since the system is simulated in transient conditions, inaccuracies in the boundary conditions propagate over time, affecting the entire simulation. For this reason, thermal validation in this work is limited to the northern section of the network.

A similar logic applies to the distribution networks. In this case, one of the many distribution networks is simulated applying the same model discussed for the transport network. This simulation allows for a more complete validation of the thermal model, due to the fact that more measurements are available at building level since they are used by the operator for billing purposes. In Figure 2, the four points adopted for the validation are reported: in these buildings, the temperature measurements are available with a time step of 10 minutes.

In this work, the analysis is carried out on one day with available measurements, specifically March 1st. The total mass flow rate in the DHS is reported in Figure 3. The figure, highlights a peculiarity of the network load profile: the presence of pronounced daily peaks, especially during morning hours. This peak is associated with the energy-saving habits common in Mediterranean regions, where heating systems in buildings are often turned off at night and reactivated early in the morning. Another relevant aspect observable in the figure is the operation of TES units: the cumulative mass flow rate associated with all TES is also shown. TES are typically charged during periods of low demand (e.g., at night or during midday valleys) and discharged during peak hours, effectively flattening the demand profile by reducing peak loads and filling valleys.

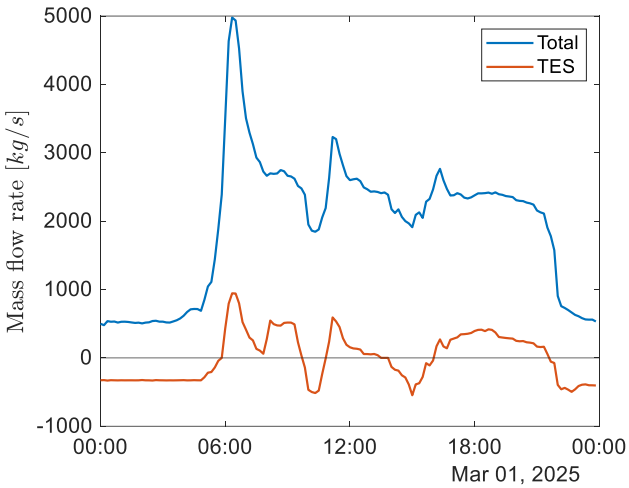

Figure 3. Daily evolution of the total mass flow rate in the DHS (blue) and of the total TES mass flow rate (red)

4. RESULTS

In this section, the results of the analysis are presented and discussed.

The application of the model to the transport network provides the distribution of mass flow rates, pressures, and temperatures throughout the network over time.

Figure 4 illustrates a representative snapshot of the thermo-fluid dynamic simulation performed on the supply line of the transport network at 08:10 AM. Similar results are available from the simulation every 10 minutes, capturing the evolution and the spatial distribution of mass flow rates and pressures throughout the network. In the figure, branch thickness is proportional to the mass flow rate, while color represents the corresponding pressure values. Higher flow rates are observed in proximity to the main generation units, located in the northern and southern sectors of the city. The pressure distribution is influenced by hydraulic losses, elevation changes, and the operation of intermediate pumping stations along the network, which may locally increase the pressure and lead to non-monotonic profiles.

Figure 5 shows the temperature distribution and mass flow rates in the supply line of the transport network at 3:50 PM. Each snapshot is extracted from the simulation results with a time step of 10 minutes. As shown in Figure 4, the branch width represents the flow rate, while the color indicates the temperature. The highest temperatures are found near the production plants, while temperature decreases gradually as water moves away from the production sites, influenced by heat losses. The areas with reduced mass flow rates are those that experience more pronounced temperature drops.

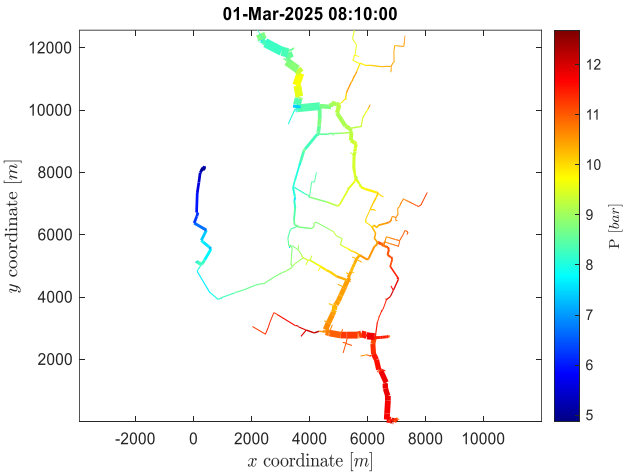

Figure 4. Results of the thermo-fluid dynamic simulation in the supply line of the transport network at 8:10 AM. (The branch width represents mass flow rates, while the color indicates pressures)

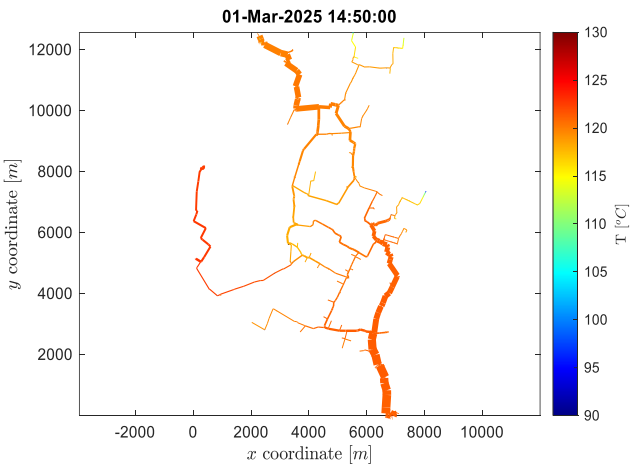

Figure 5. Results of the thermo-fluid dynamic simulation in the supply line of the transport network at 3:50 PM. (The branch width represents mass flow rates, while the color indicates temperatures)

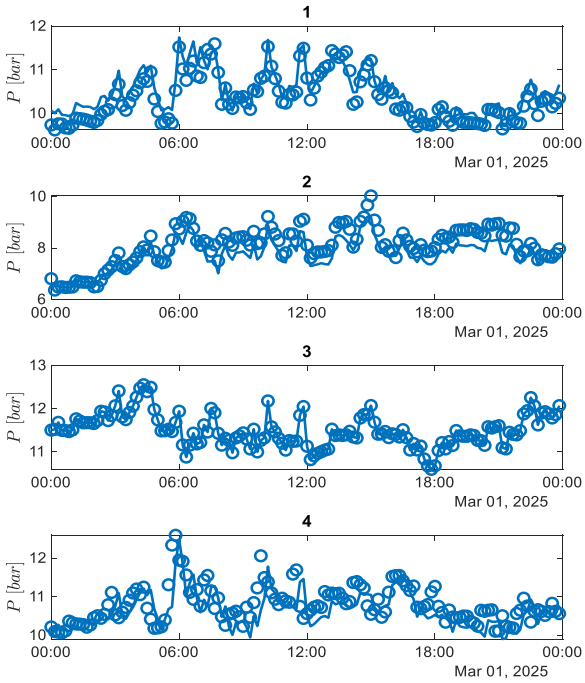

Figure 6. Comparison between experimental pressure measurements (dots) and model results (line) at four measurement locations

Figure 6 presents a comparison between experimental pressure measurements (dots) and model results (line) at four different measurement locations over the course of March 1st, 2025. The data show a generally good agreement between the model predictions and the observed pressures, demonstrating the model's ability to capture the pressure variations throughout the day. It is important to note that the pressure at location 3 is represented with high accuracy because it is used as a boundary condition in the model, rather than serving as an independent validation point. This explains the near-perfect match observed at this location, while the other locations reflect the model's predictive capabilities under varying network conditions.

Figure 7 presents a scatter plot comparing the model predictions (x-axis) against the experimental data (y-axis) for mass flow rates throughout the transport network. The bisector line represents the ideal case where the predicted and measured values perfectly match (as it occurs in location 3 that is used as boundary condition). The clustering of data points around this line indicates a good agreement between the model and experimental results. It is worth noting that in location 4, the data points form a more diffuse cloud, suggesting a slightly higher variability or uncertainty in the measurements or model predictions at this site; nevertheless, the discrepancies remain relatively low, generally below 0.5 bar. Additionally, the color gradient of the points corresponds to the ratio of local flow rate to the total flow rate, revealing that the accuracy of the model is not significantly affected by the magnitude of the flow rate. This suggests that the model's predictive capability remains consistent across the full range of flow conditions encountered in the network.

From the analysis of these results, it can be stated that the proposed fluid-dynamic model allows for an accurate estimation of pressures in a complex large-scale DHN. The model validation against pressure data on a system of this scale is a novel achievement: this work demonstrates the model robustness and applicability in large, complex transport networks. Moreover, the model runs efficiently and can be embedded within a flexible framework designed to facilitate optimization tasks, enabling straightforward application for operational and design improvements in DHS.

Figure 8 shifts the focus to temperature validation. In this case, the comparison between model predictions and experimental data is performed only at a single location, due to the limited availability of temperature measurements across the network. The results shown here indicate that the model captures well the temperature dynamics in the northern part of the network. However, some discrepancies remain, with temperature differences of up to approximately 2°C in certain instances. Despite these deviations, the model provides a satisfactory representation of the thermal behavior within the network.

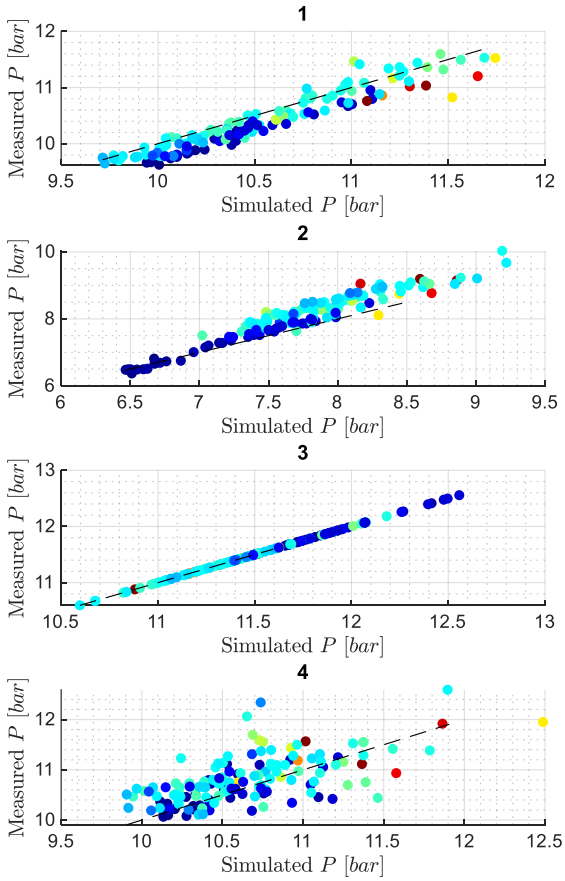

Figure 7. Comparison between pressure model results with experimental measurements at four measurement locations, for different total load values

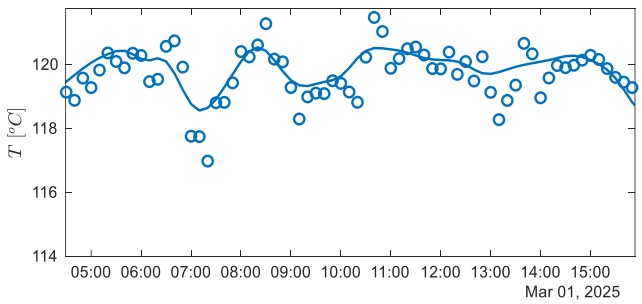

Figure 8. Comparison between experimental temperature measurements (dots) and model results (line) at one location of the transport network

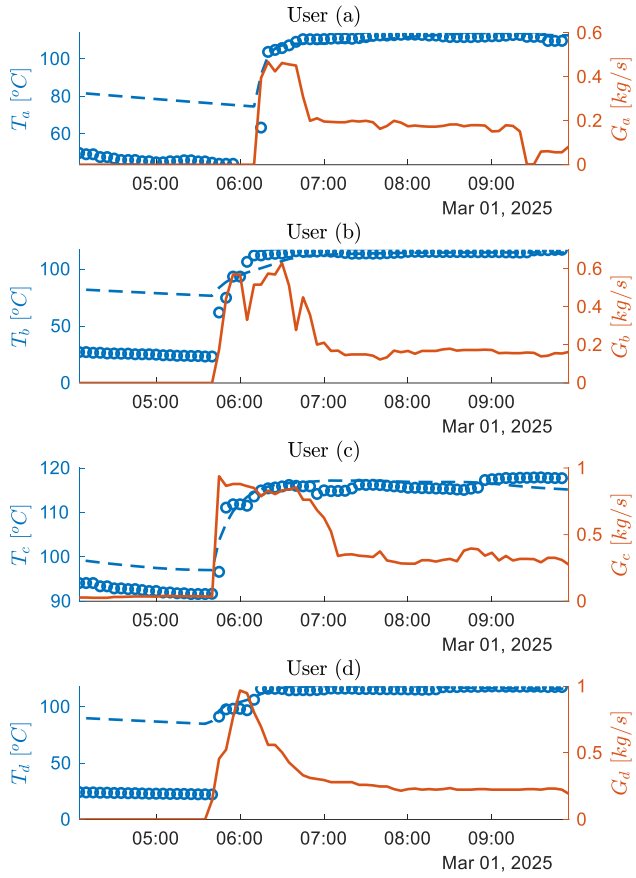

Figure 9. Comparison between experimental temperature measurements (dots) and model results (dotted line) at five substations in the distribution network

To further assess the reliability of the thermal behavior predicted by the model, the thermo-fluid dynamic simulation is also applied to a distribution network that connects the transport network to several buildings, where a greater number of measurements are available for billing purposes. The validation is carried out at four thermal substations located in different areas of the distribution network, as shown in Figure 3. The results of this validation are presented in Figure 9. In this figure, the dotted lines represent the simulated temperatures, while the dots indicate the corresponding experimental measurements. The mass flow rate required by each building is shown on the right y-axis with a continuous red line.

When the heating systems are inactive (typically during the night), the model does not accurately capture the cooling dynamics. This discrepancy arises because the experimental measurements are taken from sensors placed in the technical rooms of the buildings, which are unheated and exposed to outdoor conditions. In contrast, the model outputs refer to the temperature of the buried pipes at the building level. Additionally, the secondary circuit often remains active for a period after the primary circuit has shut down and this dynamic is not accounted for in the current model.

While these factors affect the accuracy of the measurements during periods of zero flow, they have negligible impact under normal operating conditions. In fact, during periods of active heating, when a positive mass flow rate is present, the model predictions are well aligned with the experimental data, confirming the model's ability to accurately capture the thermal dynamics of the system. It is also worth noting that only these operating conditions are truly relevant for the simulation and the thermal analysis of the network, as no thermal energy is exchanged with the network when the flow rate is zero.

Overall, it can be stated that the proposed model demonstrates a high degree of accuracy in estimating the thermal dynamics within a complex, large-scale DHS.

Based on the outcomes of the validation, it can be concluded that the thermo-fluid dynamic model presented in this work provides reliable results from both hydraulic and thermal perspectives. The successful comparison with experimental measurements at both transport and distribution levels demonstrates the capability of the model to reproduce the real behavior of the DHS under normal operating conditions. For this reason, the model can be considered validated.

Thanks to its accuracy, the model can be effectively used to analyze the current operating state of DHS. For example, it enables the quantification of pressure differentials currently guaranteed to end users, values that can be adopted as reference constraints in future optimization or reconfiguration studies. This ensures that any proposed change maintains at least the same level of service quality.

Moreover, the MIQCP feasibility framework introduced in this study can be extended into a full optimization tool by introducing additional degrees of freedom (optimization variables) and defining suitable objective functions. One ongoing line of research involves treating pump operation as an optimization variable, with the goal of identifying more efficient pumping strategies that minimize hydraulic power demand while satisfying user requirements and network constraints (e.g., pressure bounds, maximum allowable velocity). Preliminary results suggest that this approach may reduce pumping power by approximately 10%. In addition to optimization of pumping strategies, other potential applications of the proposed modeling and optimization framework include the integration of TES systems with optimized charging and discharging strategies, the integration of additional renewable energy technologies, and the analysis of reduced-temperature operation scenarios. These developments could support the transition toward more flexible, efficient, and sustainable DHS, and will be explored in future research.

5. CONCLUSIONS

This paper presents a physics-based thermo-fluid dynamic model designed to simulate the behavior of large-scale DHS under evolving operational conditions typical of the ongoing energy transition. The model solves the conservation equations of mass, momentum, and energy using a one-dimensional finite volume approach on a complex network topology, enabling accurate prediction of pressure, mass flow rate, and temperature distributions across the system.

Validation against a real DHS case study in Northern Italy demonstrated that the model can reliably reproduce the spatial and temporal dynamics of pressures and temperatures within a large and complex transport network, including multiple loops, production plants, and thermal energy storage units. Pressure predictions showed good agreement with experimental measurements across various locations and operating conditions, confirming the robustness of the fluid dynamic modeling framework. Temperature simulations also aligned well with available data, despite limited measurement

points and inherent challenges in transient thermal boundary conditions.

A key contribution of this work is the integration of the hydraulic and thermal problems into a MIQCP framework. This innovative solution approach enables efficient computation and facilitates embedding the model within optimization routines for operational and design improvements. The ability to pre-process tree-shaped network regions further enhances computational performance, making the model suitable for large-scale DHS and practical for transition scenario analyses.

Overall, the proposed framework supports the assessment and optimization of DHS with low-temperature operation and renewable integration, helping to transition from existing infrastructure to next-generation decarbonized heating networks. Future work will focus on extending the model to optimization frameworks, including optimization of pump operation and thermal storage management to further enhance system efficiency.

ACKNOWLEDGMENT

The author gratefully acknowledges the district heating operator for providing the data essential to this research.

The study developed in this paper is part of a project funded under the National Recovery and Resilience Plan (NRRP), Mission 4 Component 2 Investment 1.3 - Call for tender No. 341 of 15.03.2022 of Ministero dell'Università e della Ricerca (MUR); funded by the European Union – NextGenerationEU. Award Number: Project code PE0000021, Concession Decree No. 1561 of 11.10.2022 adopted by Ministero dell'Università e della Ricerca (MUR), CUP E13C22001890001, Project title "Network 4 Energy Sustainable Transition – NEST".

REFERENCES

[1] Lund, H., Werner, S., Wiltshire, R., Svendsen, S., Thorsen, J.E., Hvelplund, F., Mathiesen, B.V. (2014). 4th Generation District Heating (4GDH). Integrating smart thermal grids into future sustainable energy systems. Energy, 68: 1-11. https://doi.org/10.1016/j.energy.2014.02.089

[2] Werner, S. (2017). International review of district heating and cooling. Energy, 137: 617-631. https://doi.org/10.1016/j.energy.2017.04.045

[3] Østergaard, D.S., Smith, K.M., Tunzi, M., Svendsen, S. (2022). Low-temperature operation of heating systems to enable 4th generation district heating: A review. Energy, 248: 123529. https://doi.org/10.1016/j.energy.2022.123529

[4] Werner, S. (2022). Network configurations for implemented low-temperature district heating. Energy, 254: 124091. https://doi.org/10.1016/j.energy.2022.124091

[5] Sarbu, I., Mirza M., Muntean, D. (2022). Integration of renewable energy sources into low-temperature district heating systems: A review. Energies, 15(18): 6523. https://doi.org/10.3390/en15186523

[6] Guelpa, E., Capone, M., Sciacovelli, A., Vasset, N., Baviere, R., Verda, V. (2023). Reduction of supply temperature in existing district heating: A review of strategies and implementations. Energy, 262: 125363. https://doi.org/10.1016/J.ENERGY.2022.125363

[7] Capone, M., Guelpa, E., Verda, V. (2023). Potential for supply temperature reduction of existing district heating substations. Energy, 285: 128597. https://doi.org/10.1016/j.energy.2023.128597

[8] Rämä, M., Sipilä, K. (2017). Transition to low temperature distribution in existing systems. Energy Procedia, 116: 58-68. https://doi.org/10.1016/j.egypro.2017.05.055

[9] Sarbu, I., Mirza M., Crasmareanu, E. (2019). A review of modelling and optimization techniques for district heating systems. International Journal of Energy Research, 6572-6598. https://doi.org/10.1002/er.4600

[10] Ricci, M., Sdringola, P., Tamburrino, S., Puglisi, G., Donato, E.D., Ancona, M.A., Melino, F. (2022). Efficient district heating in a decarbonisation perspective: A case study in Italy. Energies, 15(3): 948. https://doi.org/10.3390/en15030948

[11] Lund, H, Østergaard, P.A., Nielsen, T.B., Werner, S., Thorsen, J.E., Gudmundsson, O., Arabkoohsar, A., Mathiesen, B.V. (2021). Perspectives on fourth and fifth generation district heating. Energy, 227: 120520. https://doi.org/10.1016/j.energy.2021.120520

[12] Pálsson, H. (2000). Methods for Planning and Operating Decentralized Combined Heat and Power Plants. Risø & DTU - Department of Energy Engineering (ET), Kgs. Lyngby, Denmark.

[13] Bøhm, B. (2000). On transient heat losses from buried district heating pipes. International Journal of Energy Research, 24: 1311-1334. https://doi.org/10.1002/1099-114X(200012)24:15%3C1311::AID-ER648%3E3.0.CO;2-Q

[14] Wallentén, P. (1991). Steady-state heat loss from insulated pipes. Licentiate Thesis, Division of Building Physics. Byggnadsfysik LTH, Lunds Tekniska Högskola.

[15] Bahlawan, H., Ferraro, N., Gambarotta, A., Losi, E., Manservigi, L., Morini, M., Saletti, C., Spina, P.R., Venturini, M. (2022). Detection and identification of faults in a district heating network. Energy Conversion and Management, 266: 115837. https://doi.org/10.1016/j.enconman.2022.115837

[16] Capone, M., Guelpa, E., Verda, V. (2023). Optimal installation of heat pumps in large district heating networks. Energies, 16(3): 1448. https://doi.org/10.3390/en16031448

[17] Bøhm, B., Ha, S., Kim, W., Kim, B., Koljonen, T., Larsen, H.V., Lucht, M., Park, Y., Sipilä, K., Wigbels, M., Wistbacka, M. (2002). Simple Models for Operational Optimisation. IEA District Heating and Cooling, Annex VI: Report 2002: S1. International Energy Agency.

[18] Dalla Rosa, A., Li, H.W., Svendsen, S. (2013). Modeling transient heat transfer in small-size twin pipes for end-user connections to low-energy district heating networks. Heat Transfer Engineering, 34(4): 372-384. https://doi.org/10.1080/01457632.2013.717048

[19] Guelpa, E., Sciacovelli, A., Verda, V. (2019). Thermo-fluid dynamic model of large district heating networks for the analysis of primary energy savings. Energy, 184: 34-44. https://doi.org/10.1016/j.energy.2017.07.177

[20] Capone, M., Guelpa, E., Verda, V. (2021). Accounting for pipeline thermal capacity in district heating simulations. Energy, 219: 119663.

https://doi.org/10.1016/j.energy.2020.119663

NOMENCLATURE

A	incidence matrix
f	known term vector
G	mass flow rate vector, $kg \cdot s^{-1}$
K	stiffness matrix
M	mass matrix
R	fluid dynamic resistance matrix
P	pressure vector, Pa
t	pumping vector
NN	number of nodes
NB	number of branches
z	altitude, m
f	friction factor
S	section, m^2
L	length, m

Greek symbols

ρ	density, $kg \cdot m^{-3}$
β	local pressure loss coefficient

Subscripts

t	time